Development of dielectric de Laval nozzles for laser electron acceleration by ultrashort pulses micromachining

Bruno Britto Chiomento
IPEN – CNEN/SP
São Paulo, SP, Brazil
bbchiomento@gmail.com

Armando V. F. Zuffi
IPEN – CNEN/SP
São Paulo, SP, Brazil
armandozuffi@gmail.com

Nilson Dias Vieira Junior
IPEN – CNEN/SP
São Paulo, SP, Brazil
nilsondiasvieirajr@gmail.com

Fabio B. D. Tabacow
IPEN – CNEN/SP
São Paulo, SP, Brazil
fabio.tabacow@gmail.com

Edson P. Maldonado
Instituto Tecnológico de Aeronáutica
São José dos Campos, SP, Brazil
puigmald@gmail.com

Ricardo Elgul Samad
IPEN – CNEN/SP
São Paulo, SP, Brazil
resamad@gmail.com

2021 SBFoton International Optics and Photonics Conference (SBFoton IOPC) | 978-1-6654-1948-2/21/$31.00 ©2021 IEEE | DOI: 10.1109/SBFOTONIOPC50774.2021.9461928

***Abstract*—This work reports the development and experimental implementation of a methodology for manufacturing submillimetric de Laval nozzles by ultrashort laser pulses micromachining by trepanning. The use of a ceramic substrate resulted in the fabrication of nozzles with high circularity and low roughness, which should generate high-quality gas targets for accelerating electrons with ultrashort laser pulses.**

Keywords—de Laval nozzles, profilometry, ultrashort laser pulses,

I. INTRODUCTION

Laser wakefield acceleration systems (LWFA) have had a rapid growth in the scientific community as a viable technology for new particle accelerator schemes [1, 2]. This technique relies on ultrashort laser pulses creating a plasma that generates acceleration gradients above 100 GV/m, much above those currently limited to the order of 100 MV/m [3] in conventional RF accelerators due to materials breakdown. These laser accelerators are smaller and less complex than their RF counterparts, reducing the costs and shielding of particle accelerators. Moreover, in this type of acceleration systems, usually renewable and fluid targets are used to create the plasma and stimulate the creation of the longitudinal electric field (wakefield) capable of accelerating electrons [4]. The interaction of particles (electrons) with matter allows the development of compact and tunable sources, which can be used in many applications as new imaging techniques [5] and for the production of medicinal radiopharmaceuticals [3, 6, 7].

Lasers with peak powers from a few TW to few PW are required to accelerate electrons [8, 9], but recent advances were obtained in the acceleration with sub-TW pulses [10-12]. These low powers can attain acceleration using high-density gas jets targets with ~100 μm thickness, which create conditions to the occurrence of Self-Modulated Laser Wakefield Acceleration (SM-LWFA) [8, 13, 14]. This regime generates highly nonlinear waves of plasma even for few mJ-class laser pulses [8, 15], and requires gas jet targets with special characteristics.

For the generation of electron beams in the SM-LWFA regime with energies up to dozens of MeV from a few mJ [12, 15], laser pulses are focused on gaseous targets, defined by a gas jet with controlled pressure, density and dimensions, expanding in a vacuum. In the target, the gas density must be as constant as possible, with values in the range of 10^{18} to 10^{21} cm^{-3} [16], being generally delivered in high-density supersonic jets, pulsed synchronously with the laser [17]. To obtain uniform supersonic beams with a well-defined density transition region, de Laval nozzles [18-20] are used. This type of nozzle, shown schematically in Fig. 1, is defined by a constriction region, a throat that strangles the gas flow with a minimum (throat) radius r_t, and an expanding outlet section ending with an opening with radius r_e. If enough pressure difference exists between the backing and experimental chambers (Fig. 1), the gas velocity locally becomes sonic at the minimum cross-section position. As the nozzle cross-section increases along the exit cone, the gas undergoes an adiabatic expansion and the flow increases to supersonic. The molecules at supersonic speeds have a low transverse speed [18], with sharp jet-vacuum boundaries and flattened (approximately constant) gas density profiles. These characteristics are of utmost importance to obtain SM-LWFA.

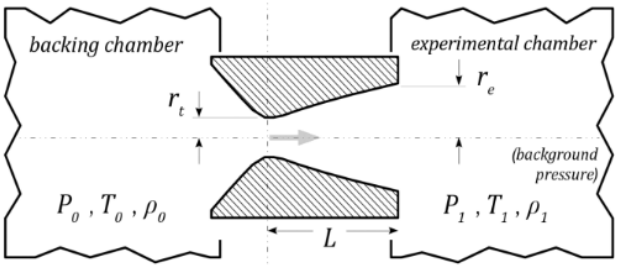

Fig. 1. Scheme of a de Laval nozzle. The throat radius is r_t, the exit radius r_e, and L is the length of the conical exit section. P, T and ρ are the gas pressure, temperature and density.

Two limit cases exist: the sonic nozzle, in which the radii of the throat and the exit are the same ($r_e = r_t$), and the supersonic nozzle, in which the radius of the outlet is greater than that of the throat ($r_e > r_t$). In both geometries the flow is always sonic (or choked) in the throat section and acceleration occurs at the exit.

The flow will only be choked in the throat if the ratio between the upstream pressure (in the backing chamber) and the downstream pressure (in the experimental chamber) is above a certain value (usually around 2), sufficient to produce sonic velocities at the throat, otherwise the supersonic flow will not be obtained. Since the mass flow through the nozzle is constant, as the cross-sectional area is

This work was supported by FAPESP, SAE and CNPq.

enlarged the axial velocity has to become progressively more supersonic. The design of the jet's Mach number is optimized for the type of experiment, its objectives, available laser parameters (peak power, beam focus area, pulse duration and energy), and pressure in the gas chamber.

A commonly used quasi-1D model of the de Laval nozzle [21] assumes an isentropic flow and produces useful expressions for the mass flow rate, $\dot{m}$, (1), Mach number M as a function of the exit to throat area ratio, A_e/A_t, (2), divergence angle for vacuum-quality background pressure, α, (3) and maximum jet gas density, ρ, (4):

$$\dot{m} = A_t P_0 \sqrt{\frac{\gamma}{R T_0}} \left(\frac{2}{\gamma+1} \right)^{\frac{\gamma+1}{2(\gamma-1)}} \quad (1)$$

$$\frac{A_e}{A_t} = \frac{1}{M} \left[\frac{2+(\gamma-1)M^2}{\gamma+1} \right]^{\frac{\gamma+1}{2(\gamma-1)}} \quad (2)$$

$$\alpha = 1/M \quad (3)$$

$$\frac{\rho}{\rho_0} = \frac{1}{M} \left[\frac{\gamma+1}{2+(\gamma-1)M^2} \right]^{\frac{1}{(\gamma-1)}}, \quad (4)$$

where ρ and ρ_0 are the jet and backing reservoir densities, respectively, P_0 and T_0 are the reservoir pressure and temperature, γ is the heat capacity ratio, or adiabatic index and R is the specific gas constant. This model disregards the exact value of the background density, the presence of shock waves, as well as the nozzle length, L, and other geometrical features like the length of the converging region, shapes and curvatures, all these affecting the jet discharge and speed (and pressure) as second-order corrections [21].

We are working to implement SM-LWFA in our laboratory, and for that we are fabricating our own de Laval nozzles by ultrashort laser pulses micromachining [22].

Machining by femtosecond pulses is usually known as athermal machining [23-25] for producing a heat affected zone below 1 µm. The interaction of femtosecond pulses with matter occurs through non-linear ionizations [26, 27] that create a cloud of free electrons, which upon relaxing its energy to the matrix, produces a phase explosion that removes material [26-28]. This interaction with electrons makes ablation by ultrashort pulses non-selective, occurring in any material, and its non-thermal character allows micrometric structures to be machined with high precision [29, 30]. These characteristics make ablation by ultrashort pulses ideal for machining gas nozzles in metals and in dielectrics.

We started manufacturing de Laval nozzles in our laboratory [22] by using ultrashort laser pulses (25 fs, 785 nm, 100-600 µJ) drilling 0.5 mm metal plates by percussion [22, 29], and typical nozzle exit and throat machined are shown in Fig. 2. This figure presents topographic maps obtained by an optical profiler (ZeGage, Zygo), and it can be seen that the holes do not have cylindrical symmetry, mainly in the nozzle throat. These asymmetries arise from inhomogeneities in the laser profile and the low ablation threshold of metals [31], which make them very sensitive to laser intensity fluctuations.

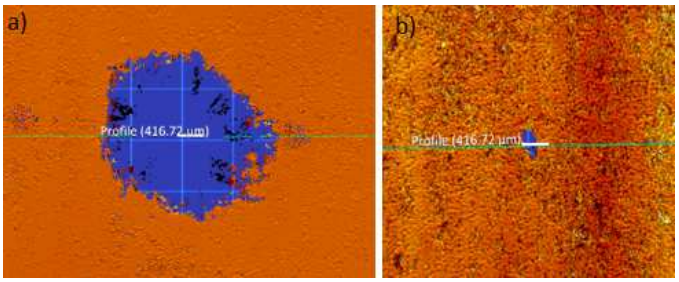

Fig. 2. Nozzle drilled by 150 µJ pulses in a copper plate by percussion. a) nozzle exit with ~220 µm diameter; b) nozzle throat with ~10 µm diameter.

The results shown in Fig. 2 lead us to look for other ways to laser machine nozzles aiming to get more circular holes. This was obtained modifying the machining process from percussion to trepanning [29, 32], and replacing the material by a dielectric.

II. METHODOLOGY

The Ti:sapphire CPA laser system used for machining the de Laval nozzles (Femtolasers Femtopower Compact Pro HR/HP) produces 25 fs (FWHM) pulses centered at 785 nm with 40 nm of bandwidth (FWHM), up to 650 µJ, at 4 kHz repetition rate, producing a laser beam with M^2 factor of 1.5. The ultrashort pulses are directed to the machining area, and are focused by an achromatic doublet, whose focal length depends on the characteristics of the desired nozzle. Typical focal values are 30, 50.4 and 75 mm, and the results presented here, obtained with the 30 mm lens are representative for the other lenses also. The laser beam diameter at the lens is 8 mm, and we estimated the focused beamwaist to be ~10 µm due to residual chromatic and spherical aberrations. With these considerations, the confocal parameter of the beam is ~500 µm, being adequate to drill substrates with similar thicknesses. The beam is focused on the surface of a 600 µm thick alumina (Al_2O_3) plate that is attached to a mount connected to a rotating electric motor, as shown in Fig. 3, coupled to computer-controlled micrometric positioning system that moves the sample in the focal plane of the lens. The motor rotates at a 20-30 RPM. The focused beam propagation direction is parallel to the rotating motor axis, and adjusting the distance between them with the translating stage defines the nozzle exit diameter. The lens numerical aperture determines the nozzle walls angle, and consequently, the throat radius. As the most important parameter to define the Mach number of a gas jet is the ratio between the areas of the throat and the exit of the gas nozzle, as exposed by (2), combining the lens and the laser beam distance to the rotation axis give us flexibility to choose the nozzle Mach. The choice of the focusing lens is given according to its numerical aperture [13], which on first approximation defines the inclination of the gas nozzle walls and defines the sizes of the throat and the gas outlet.

After the nozzle is etched, the beam is moved 1 mm laterally, and the laser cuts a 2 mm diameter disk, which has the nozzle at its center. This disk is glued to the tip of a metal part that connects to the gas line, as show in Fig. 4. This part has a 1 mm hole through it, defining the backing chamber.

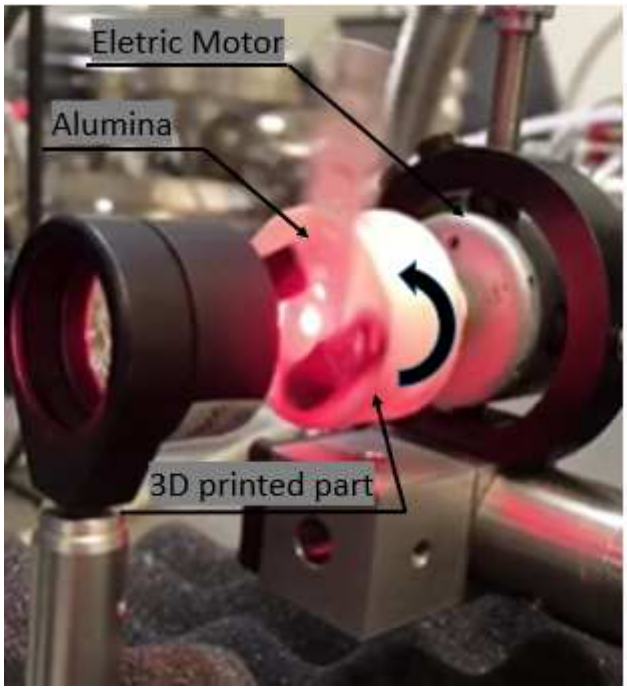

Fig. 3. Alumina plate coupled to the micromachining rotary system (electric motor with 3D printed part).

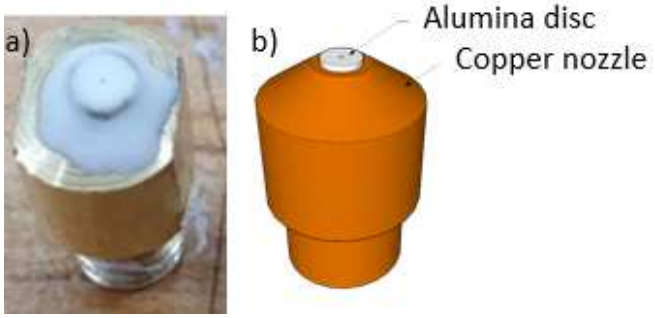

Fig. 4. a) de Laval nozzle used in the experiment. b) 3D scheme of the alumina disk containing the de Laval Nozzle coupled to the beak.

III. Results

The trepanning method moves the substrate being machined relative to the laser beam, which is used as a cutting tool. This homogenizes the etching because the exact shape of the beam (and its inhomogeneities) just determines the cutting kerf. These characteristics, allied to the use of alumina, a dielectric with an ablation threshold an order of magnitude above that of metals, make the etching less sensitive to intensity fluctuations and beam displacements. The nozzle cylindrical symmetry is then defined by the rotation of the substrate relative to the laser beam, and not by its intensity profile.

Fig. 5 exhibits the results of a submillimetric nozzle fabricated by the described technique with 350 µJ pulses focused by the 30 mm focal length lens, with 4 kHz repetition rate. Figs. 5a and 5b present profile maps of the nozzle exit and throat, respectively, and a high circularity can be observed in both cases, mainly in the nozzle exit. The use of the measured exit and throat diameters of ~290 µm and ~60 µm, respectively, in (2) results in an estimated Mach number of ~4.5 when using N_2 (γ=1.47).

From the Scanning Electron Micrography (SEM) of the nozzle exit shown in Fig. 5c, which presents the nozzle walls, it is possible to observe that their roughness is smaller than that of the alumina surface. This is a result from melting and ressolidification of the alumina [33, 34] that occurs as a consequence of the elevated pulse energy and high repetition rate, which lead to sufficient heat accumulation to promote melting and ressolidification [34], while maintaining a small heat-affected zone. This ressolidification [35] fuses the ceramic (alumina) grains, producing smooth walls with reduced roughness relatively to the starting material.

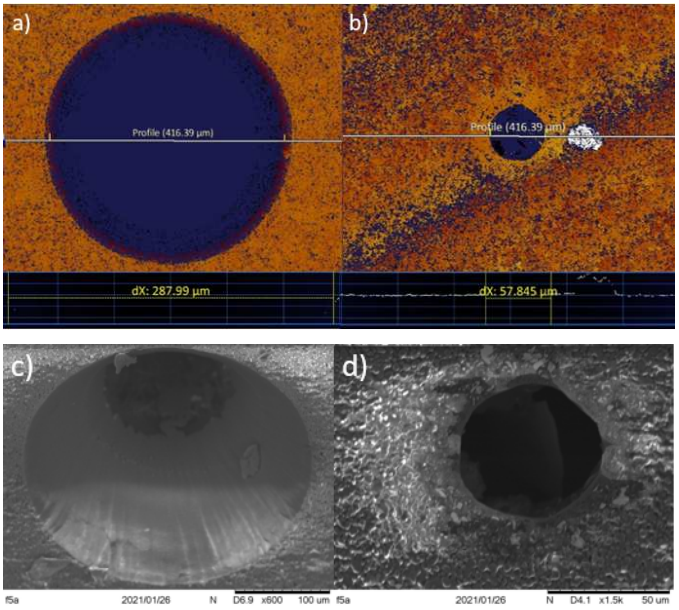

Fig. 5. a) nozzle outlet profilometry b) nozzle throat profilometry c) nozzle outlet SEM d) nozzle throat SEM.

We expect that the nozzles high circularity and small roughness (whose value could not be measured for the lack of a suitable method, which we are developing) generate very symmetrical and laminar gas flows that will be used as targets. These targets will be characterized by schlieren imaging and interferometry [22], and the gas flow through nozzles will be simulated by Computational Fluid Dynamics [36], and the experimental and theoretical results will be used to provide feedback to the manufacturing process to create nozzles and targets optimized for SM-LWFA.

IV. Conclusions

Using a new machining method and replacing metal by a dielectric, we improved the quality and control of submillimetric de Laval nozzles etched by ultrashort laser pulses. The nozzles high circularity and small roughness are expected to generate improved gas targets to accelerate electrons with ultrashort laser pulses.

Acknowledgment

The authors would like to acknowledge the financial support from FAPESP, CNPq, and B. B. Chiomento and Armando V. F. Zuffi thank CAPES and CNPq for their scholarships.

References

[1] T. Katsouleas, "Accelerator physics - Electrons hang ten on laser wake," Nature, vol. 431, pp. 515-516, 2004.

[2] T. Tajima, K. Nakajima, and G. Mourou, "Laser acceleration," Riv Nuovo Cimento, vol. 40, pp. 33-U102, 2017.

[3] A. Giulietti, Laser-Driven Particle Acceleration Towards Radiobiology and Medicine, Springer International Publishing, 2016, pp.

[4] E. Esarey, C.B. Schroeder, and W.P. Leemans, "Physics of laser-driven plasma-based electron accelerators," Rev Mod Phys, vol. 81, pp. 1229-1285, 2009.

[5] F. Albert, "Laser Wakefield Accelerators: Next-Generation Light Sources," Optics and Photonics News, vol. 29 (January 2018), pp. 42-49, 2018.

[6] K. Nemoto, "Laser-triggered ion acceleration and table top isotope production," Appl Phys Lett, vol. 78, pp. 595-597, 2001.

[7] I. Spencer, "Laser generation of proton beams for the production of short-lived positron emitting radioisotopes," Nucl Instrum Meth B, vol. 183, pp. 449-458, 2001.

[8] J. Faure, "A review of recent progress on laser-plasma acceleration at kHz repetition rate," Plasma Phys Contr F, vol. 61, pp., 2019.

[9] S. M. Hooker, "Developments in laser-driven plasma accelerators," Nat Photonics, vol. 7, pp. 775-782, 2013.

[10] A. J. Goers, "Multi-MeV Electron Acceleration by Subterawatt Laser Pulses," Phys Rev Lett, 115, pp., 2015.

[11] S. Masuda, and E. Miura, "Generation and analysis of quasimonoenergetic electron beams by laser-plasma interaction in transitional region from the self-modulated laser wakefield to bubble acceleration regime," Physics of Plasmas, vol. 16, pp., 2009.

[12] B. Hidding, "Quasimonoenergetic electron acceleration in the self-modulated laser wakefield regime," Physics of Plasmas, vol. 16, pp., 2009.

[13] C. Y. Hsieh, M. W. Lin, and S.H. Chen, "Simulation study of the sub-terawatt laser wakefield acceleration operated in self-modulated regime," Physics of Plasmas, vol. 25, pp., 2018.

[14] N. Lemos, "Self-modulated laser wakefield accelerators as x-ray sources," Plasma Phys Contr F, vol. 58, pp., 2016.

[15] F. Salehi, "MeV electron acceleration at 1 kHz with <10 mJ laser pulses," Opt. Lett., vol. 42, pp. 215-218, 2017.

[16] W. P. Leemans, "Laser-driven plasma-based accelerators: Wakefield excitation, channel guiding, and laser triggered particle injection," Physics of Plasmas, vol. 5, pp. 1615-1623, 1998.

[17] K. Schmid, and L. Veisz, "Supersonic gas jets for laser-plasma experiments," Rev Sci Instrum, vol. 83, pp. 053304, 2012.

[18] K. Foelsch, "The Analytical Design of an Axially Symmetric Laval Nozzle for a Parallel and Uniform Jet," J Aeronaut Sci, vol. 16, pp. 161-&, 1949.

[19] F. Rodriguez, "Laval nozzle flow characterization by Fourier-transform Mach-Zehnder interferometry," in Optical Measurement Systems for Industrial Inspection IV, Pts 1 and 2, Osten, W., Gorecki, C. and Novak, E. Eds. Bellingham: Spie-Int Soc Optical Engineering, 2005, pp. 865-873.

[20] S. Lorenz, "Characterization of supersonic and subsonic gas targets for laser wakefield electron acceleration experimentsx," Matter Radiat Extrem, vol. 4, pp., 2019.

[21] F. Sylla, M. Veltcheva, S. Kahaly, A. Flacco, and V. Malka, "Development and characterization of very dense submillimetric gas jets for laser-plasma interaction," Rev Sci Instrum, vol. 83, pp. 033507, 2012.

[22] R R. E. Samad, A. V. F. Zuffi, E. P. Maldonado, and N. D. Vieira : 'Development and Optical Characterization of Supersonic Gas Targets for High-Intensity Laser Plasma Studies', in in 2021 SBFoton International Optics and Photonics Conference (SBFoton IOPC), 2018.

[23] A. V. Lugovskoy, and I. Bray, "Ultrafast electron dynamics in metals under laser irradiation," Physical Review B, vol. 60, pp. 3279-3288, 1999.

[24] M. D. Perry, "Ultrashort-pulse laser machining of dielectric materials," Journal of Applied Physics, vol. 85, pp. 6803-6810, 1999.

[25] J. Cheng, "A review of ultrafast laser materials micromachining," Optics & Laser Technology, vol. 46, pp. 88-102, 2013.

[26] D. Ashkenasi, M. Lorenz, R. Stoian, and A. Rosenfeld, "Surface damage threshold and structuring of dielectrics using femtosecond laser pulses: the role of incubation," Appl. Surf. Sci., vol. 150, pp. 101-106, 1999.

[27] N. M. Bulgakova, and I. M. Bourakov, "Phase explosion under ultrashort pulsed laser ablation: modeling with analysis of metastable state of melt," Appl. Surf. Sci., vol. 197, pp. 41-44, 2002.

[28] P. Lorazo, L. Lewis, and M. Meunier, "Short-Pulse Laser Ablation of Solids: From Phase Explosion to Fragmentation," Phys. Rev. Lett., vol. 91, pp., 2003.

[29] S. Mishra, and V. Yadava, "Laser Beam MicroMachining (LBMM) – A review," Opt. and Las. in Eng., vol. 73, pp. 89-122, 2015.

[30] M. P. Raele, L. R. De Pretto, W. de Rossi, N. D. Vieira, and R. E. Samad, "Focus Tracking System for Femtosecond Laser Machining using Low Coherence Interferometry," Sci. Rep., 9, pp. 4167, 2019.

[31] S. Nolte, "Ablation of metals by ultrashort laser pulses," Journal of the Optical Society of America B-Optical Physics, vol. 14, pp. 2716-2722, 1997.

[32] A. Tuennermann, S. Nolte, and J. Limpert, "Femtosecond vs. Picosecond Laser Material Processing," Laser Technik Journal, vol. 7, pp. 34-38, 2010.

[33] Q. T. Le, C. Bertrand, and R. Vilar, "Femtosecond laser ablation of enamel," Journal of biomedical optics, vol. 21, pp. 65005, 2016.

[34] M. Garcia-Lechuga, J. Solis, and J. Siegel, "Melt front propagation in dielectrics upon femtosecond laser irradiation: Formation dynamics of a heat-affected layer," Appl. Phys. Lett., 108, pp. 171901, 2016.

[35] B. Nie, H. Huang, S. Bai, and J. Liu, "Femtosecond laser melting and resolidifying of high-temperature powder materials," Appl. Phys. A-Mat. Sci. Proc., vol. 118, pp. 37-41, 2014.

[36] F. B. D. Tabacow, A. V. F. Zuffi, E. P. Maldonado, R. E. Samad, and N. D. Vieira, "Theoretical and experimental study of supersonic gas jet targets for laser wakefield acceleration," in 2021 SBFoton International Optics and Photonics Conference (SBFoton IOPC), in press.